



**Photochemical intermediates of trans-Rh(CO)L<sub>2</sub>Cl  
where L=PMe<sub>3</sub>, PBu<sub>3</sub>, and i-Pr<sub>2</sub>HN and  
cis-Rh(CO)<sub>2</sub>(i-Pr<sub>2</sub>HN)Cl in frozen organic glasses**

Thomas Bitterwolf, W.Bruce Scallorn, J.Timothy Bays, Callie Weiss, John Linehan, James Franz, Rinaldo Poli

► **To cite this version:**

Thomas Bitterwolf, W.Bruce Scallorn, J.Timothy Bays, Callie Weiss, John Linehan, et al.. Photochemical intermediates of trans-Rh(CO)L<sub>2</sub>Cl where L=PMe<sub>3</sub>, PBu<sub>3</sub>, and i-Pr<sub>2</sub>HN and cis-Rh(CO)<sub>2</sub>(i-Pr<sub>2</sub>HN)Cl in frozen organic glasses. Journal of Organometallic Chemistry, 2002, 652 (1-2), pp.95-104. 10.1016/S0022-328X(02)01312-8 . hal-03284218

**HAL Id: hal-03284218**

**<https://hal.science/hal-03284218>**

Submitted on 20 Jul 2021

**HAL** is a multi-disciplinary open access archive for the deposit and dissemination of scientific research documents, whether they are published or not. The documents may come from teaching and research institutions in France or abroad, or from public or private research centers.

L'archive ouverte pluridisciplinaire **HAL**, est destinée au dépôt et à la diffusion de documents scientifiques de niveau recherche, publiés ou non, émanant des établissements d'enseignement et de recherche français ou étrangers, des laboratoires publics ou privés.

# Photochemical intermediates of trans-Rh(CO)L<sub>2</sub>Cl where L = PMe<sub>3</sub>, PBu<sub>3</sub>, and i-Pr<sub>2</sub>HN and *cis*-Rh(CO)<sub>2</sub>(i-Pr<sub>2</sub>HN)Cl in frozen organic glasses

Thomas E. Bitterwolf<sup>a,\*</sup>, W. Bruce Scallorn<sup>a</sup>, J. Timothy Bays<sup>a</sup>, Callie A. Weiss<sup>a</sup>, John C. Linehan<sup>b</sup>, James Franz<sup>b</sup>, Rinaldo Poli<sup>c</sup>

<sup>a</sup> Department of Chemistry, University of Idaho, Moscow, ID 83844-2343, USA

<sup>b</sup> Chemical Sciences Department, Pacific Northwest National Laboratory, PO Box 999, Richland, WA 99352, USA

<sup>c</sup> Laboratoire de Synthèses et d'Electrosynthese Organometalliques, Université de Bourgogne Faculté de Sciences "Gabriel", 21100 Dijon, France

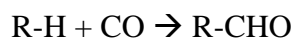
## Abstract

The Nujol glass matrix photolyses of Rh(CO)(PMe<sub>3</sub>)<sub>2</sub>Cl (**1**), Rh(CO)(PBu<sub>3</sub>)<sub>2</sub>Cl (**2**), Rh(CO)<sub>2</sub>(i-Pr<sub>2</sub>HN)Cl (**3**), and Rh(CO)(i-Pr<sub>2</sub>HN)<sub>2</sub>Cl (**4**), have been examined. Photolysis of **1** ( $\lambda_{\text{irr}} > 400$  nm) and **2** ( $350 < \lambda_{\text{irr}} < 400$  nm) give new species, **A**, with carbonyl stretching bands slightly below the parent bands. In the case of **1** this species appears to give rise to a second product, **C**, upon either extended photolysis or annealing. High-energy photolysis of **1**, **2**, and **4**, result in loss of CO and formation of an IR silent species, RhL<sub>2</sub>Cl. In the case of **1** a new carbonyl species, **B**, is observed upon high-energy photolysis or annealing of a matrix containing CO and Rh(PMe<sub>3</sub>)<sub>2</sub>Cl. **B** may be converted to **1** by either back photolysis or annealing. Compound **3** undergoes photochemical CO-loss to form two isomeric photoproducts. Comparison of the carbonyl stretching frequencies of phosphine and ammine derivatives and photoproducts made it possible to eliminate PR<sub>3</sub> loss as the source of **A**. DFT calculations suggest that **A** may be a non-planar, triplet excited state of **1** or **2**. DFT calculations also support the assignment of **B** to *cis*-Rh(CO)(PMe<sub>3</sub>)<sub>2</sub>Cl.

Keywords: Photolysis; Amine derivatives; DFT analysis

## 1. Introduction

The recent simultaneous publication of photochemical strategies for the carbonylation of ethane [1] and methane [2] using *trans*-Rh(CO)(PMe<sub>3</sub>)<sub>2</sub>Cl in supercritical CO<sub>2</sub> (sc-CO<sub>2</sub>) attests to a continuing interest in the utilization of rhodium(I) photocatalysts to carry out fundamental chemical transformations on hydrocarbon substrates. Photoassisted carbonylation of C-H bonds in aromatic hydrocarbons and alkanes has been reported by Fisher and Eisenberg [3], Tanaka and coworkers [4], Browse and Goldman [5] and their coworkers. For benzene, Reaction (1) has been shown to be catalyzed by a number of metal carbonyl phosphine compounds including IrH<sub>3</sub>(CO)(dppe) [3a,3c], Ir(CO)(PPh<sub>3</sub>)<sub>2</sub>Cl [3b,3c], Rh(CO)(PPh<sub>3</sub>)<sub>2</sub>Cl [3b,3c], Rh(CO)(PPh<sub>3</sub>)<sub>2</sub>H [3b,3c], Rh(CO)(PMe<sub>3</sub>)<sub>2</sub>Cl [4,5] and Ru(CO)<sub>4</sub>(PPh<sub>3</sub>) [3d].



Reaction (1)

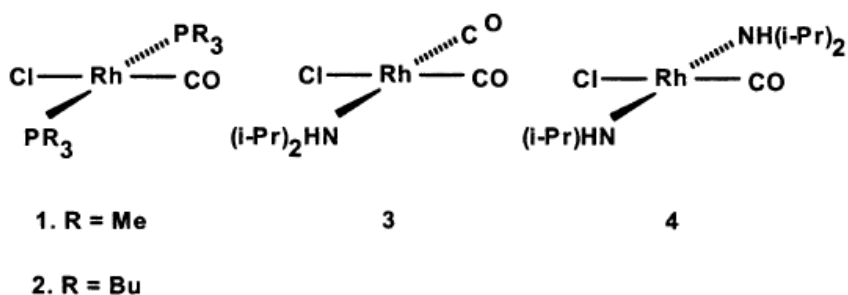
In the absence of CO, *trans*-Rh(CO)(PMe<sub>3</sub>)<sub>2</sub>Cl (**1**), catalyzes the thermodynamically unfavorable dehydration of alkanes. Goldman and coworkers [6] have examined the mechanism of this reaction and developed convincing evidence that the photolysis ( $\lambda_{\text{irr}} = 3669 \pm 20$  nm) results in CO-loss to form [Rh(PMe<sub>3</sub>)<sub>3</sub>Cl], proposed to be the active intermediate in the dehydrogenation process.

Detailed mechanistic studies by Ford and co-workers [7] and Rosini et al. [8] have established that there may be two pathways for these carbonylation reactions. One pathway involves loss of CO forming [Rh(PMe<sub>3</sub>)<sub>2</sub>Cl] that can undergo C-H insertion and subsequent CO recapture to yield a hexacoordinate species of the general form Rh(CO)(H)(R)(PMe<sub>3</sub>)<sub>2</sub>Cl. A second pathway appears to involve direct reaction of substrate with an excited state of **1** to yield the same intermediate. A secondary photochemical step initiates loss of RCHO from the

hexacoordinate intermediate. There is a marked wavelength dependence for the two oxidative addition pathways with CO-loss requiring lower energies. At a photolysis wavelength of 355 nm both pathways appear to be operative although the partitioning between the two pathways is not known.

Tanaka and co-workers [4a,4b] have reported a wavelength dependent product distribution in the photolysis of **1** with toluene and decane. High-energy light ( $\lambda_{\text{irr}} > 295$  nm) results primarily in *meta* and *para* substitution of toluene and terminal carbonylation of decane. In contrast, lower energy photolysis ( $\lambda_{\text{irr}} > 375$  nm) results in substantial methyl carbonylation of toluene and internal carbonylation of decane. It is not presently known whether the difference in product distribution is in some way related to the two oxidative addition pathways noted above.

Our long-standing interest in the identification of photochemical intermediates in frozen organic glasses prompted us to initiate what was expected to be a short investigation into the photochemistry of **1**. The results of what ultimately proved to be a multi-year odyssey are reported in this paper.



## 2. Results

Experimental procedures for photochemical studies in frozen organic glasses have been previously reported [9]. A variety of optical filters were used to control the incident light during

photochemical experiments. Compounds **1** [8], *trans*-Rh(CO)(PBU<sub>3</sub>)<sub>2</sub>Cl (**2**) [10], and *cis*-Rh(CO)<sub>2</sub>(*i*-Pr<sub>2</sub>HN)Cl (**3**) [11], were prepared by standard literature methods. *trans*-Rh(CO)(*i*-Pr<sub>2</sub>HN)<sub>2</sub>Cl (**4**), was prepared by photolysis of **3** in heptane with an excess of *i*-Pr<sub>2</sub>HN. Details of this synthesis will be reported in a subsequent publication [12].

Compound **1** is only moderately soluble in Nujol at room temperature. Samples were prepared by grinding a few crystals of **1** with Nujol followed by lengthy centrifugation to separate fine crystallites. IR spectra of the resulting solutions both at room temperature and at ca. 90 K had single, sharp lines for the carbonyl stretching band of **1** characteristic of Nujol solutions and not the broad bands typical of mulls. Nujol glass solutions of **1** at ca. 90 K are found to have two absorption bands at 360 and 275 nm (Fig. 1). At room temperature these bands are considerably broadened. Neither IR nor UV-vis spectra contained any bands that might be attributed to d-d stacked dimers or oligomers.

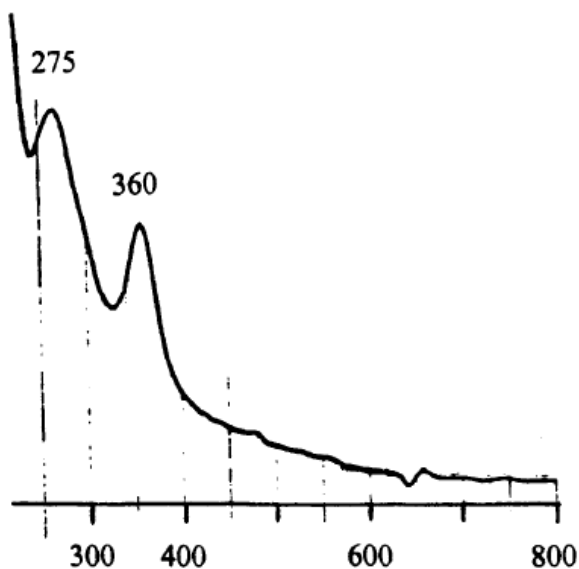


Fig. 1. Electronic spectrum of **1** in Nujol at ca. 90 K. The small features at 475 and 650 nm are instrument artifacts.

Photolysis of Nujol glass solutions of **1** at  $\lambda_{\text{irr}} > 450$  nm resulted in no detectable changes in the IR spectrum. Photolysis at  $\lambda_{\text{irr}} = 4009 \pm 70$  nm resulted in a decrease in the intensity of the band of **1** at  $1964 \text{ cm}^{-1}$  and growth of a new band at  $1955 \text{ cm}^{-1}$ . Upon extended photolysis ( $\lambda_{\text{irr}} \geq 400$  nm, 6 h) a low, broad band may be discerned at about  $1938 \text{ cm}^{-1}$  (Fig. 2a). No band for ‘free’ CO ( $21319 \pm 2 \text{ cm}^{-1}$ ) is observed at these photolysis wavelengths even after very long photolyses. Annealing a sample photolyzed in this manner to 153 K resulted in decrease of the  $1955 \text{ cm}^{-1}$  band, growth of the band at  $1964 \text{ cm}^{-1}$  and small growth in the band at  $1938 \text{ cm}^{-1}$  (Fig. 2b).

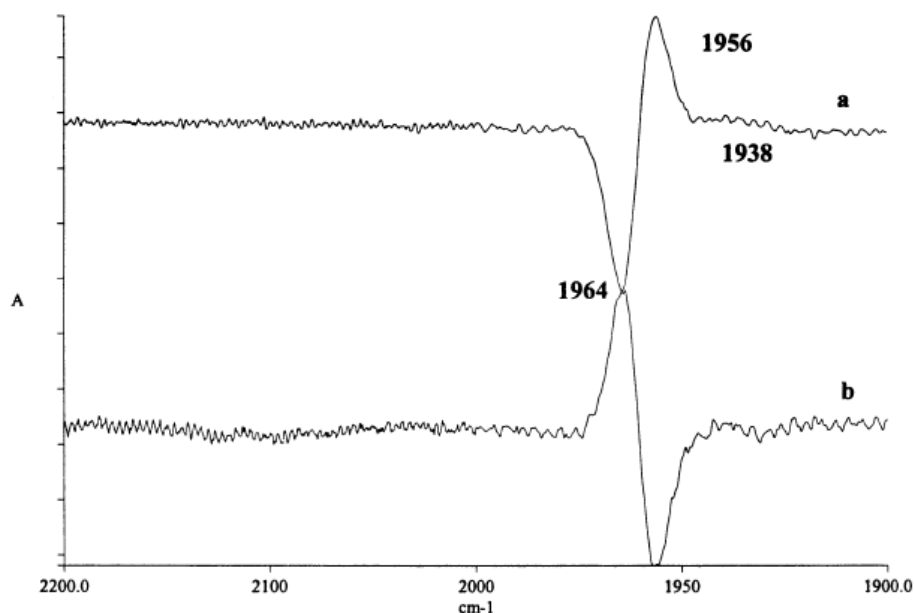


Fig. 2. (a) 6 h photolysis of **1**,  $\lambda_{\text{irr}} > 400$  nm. (b) Anneal of sample to 153 K.

Photolysis of a fresh sample of **1** ( $330 < \lambda_{\text{irr}} < 400$  nm, 1 h) results in a decrease in the carbonyl band of **1** and growth of bands at  $2131$ ,  $2012$ ,  $1954$ , and  $1938 \text{ cm}^{-1}$  (Fig. 3a). Photolysis of a fresh sample of **1** ( $\lambda_{\text{irr}} = 280 \pm 10$  nm, 30 min) resulted in decrease in the band of **1** and growth of bands at  $2131$  and  $2012 \text{ cm}^{-1}$  (Fig. 4a). Back photolysis of this sample ( $\lambda_{\text{irr}} = 450 \pm 70$  nm, 10 min) resulted in a bleaching of the band at  $2012 \text{ cm}^{-1}$  and growth of a band at  $1962 \text{ cm}^{-1}$  presumed to be **1**, with a low energy shoulder at  $1955 \text{ cm}^{-1}$  (Fig. 4b). The band at  $1955 \text{ cm}^{-1}$  may

be a result of direct photolysis of **1** at this wavelength and not be related to the back photolysis of the 2012  $\text{cm}^{-1}$  band.

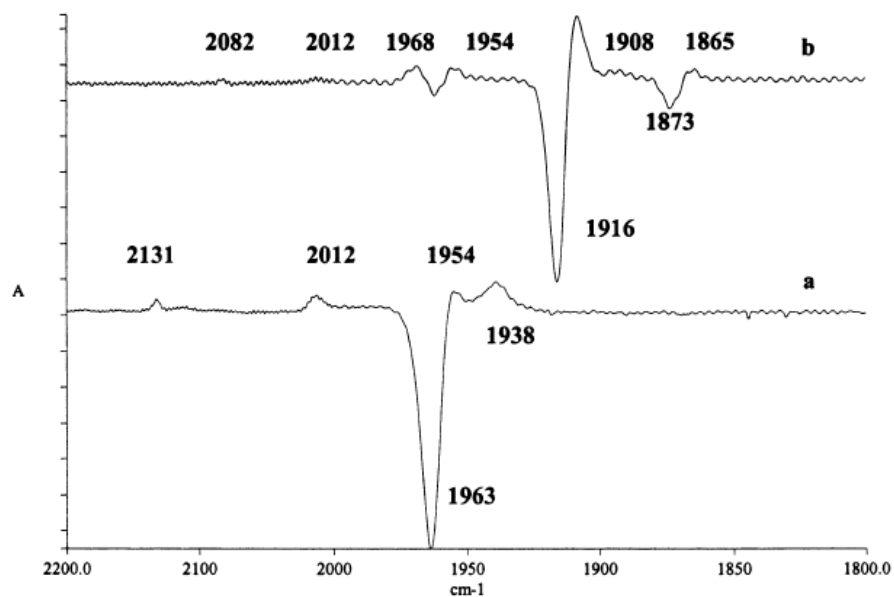


Fig. 3. (a) 1 h photolysis of **1**,  $330 < \lambda_{\text{irr}} < 400$  nm. (b) 15 min photolysis of  $^{13}\text{CO}$  labeled **1**,  $330 < \lambda_{\text{irr}} < 400$  nm.

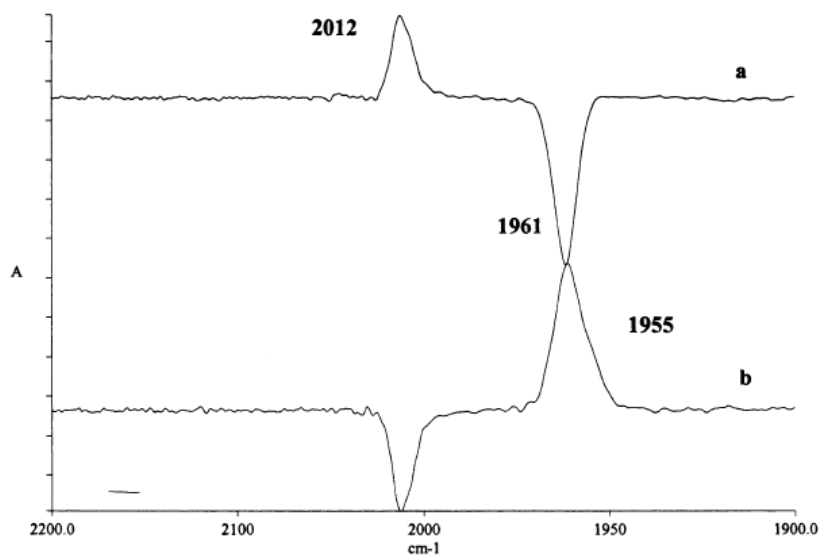


Fig. 4. (a) 30 min photolysis of **1**,  $\lambda_{\text{irr}} = 280 \pm 10$  nm. (b) 10 min back photolysis,  $\lambda_{\text{irr}} = 450 \pm 70$  nm.

Annealing studies of a sample of **1** that had been photolyzed for an extended time ( $\lambda_{\text{irr}} = 280 \pm 10$  nm, 4.5 h) were particularly informative. As before, photolysis resulted in a decrease in the band of **1** and growth of bands at 2131 and 2012  $\text{cm}^{-1}$  (Fig. 5a). Annealing this sample to 130 K resulted in a decrease in the band at 2131 and a previously unseen band at 1955  $\text{cm}^{-1}$  and growth of bands at 2012, 1964, and 1938  $\text{cm}^{-1}$  (Fig. 5b). Further annealing to 170 K resulted in further decrease in the bands at 2131 and 1955  $\text{cm}^{-1}$  as well as a decrease in the band at 2012  $\text{cm}^{-1}$  and growth of the bands at 1964 and 1938  $\text{cm}^{-1}$  (Fig. 5c).

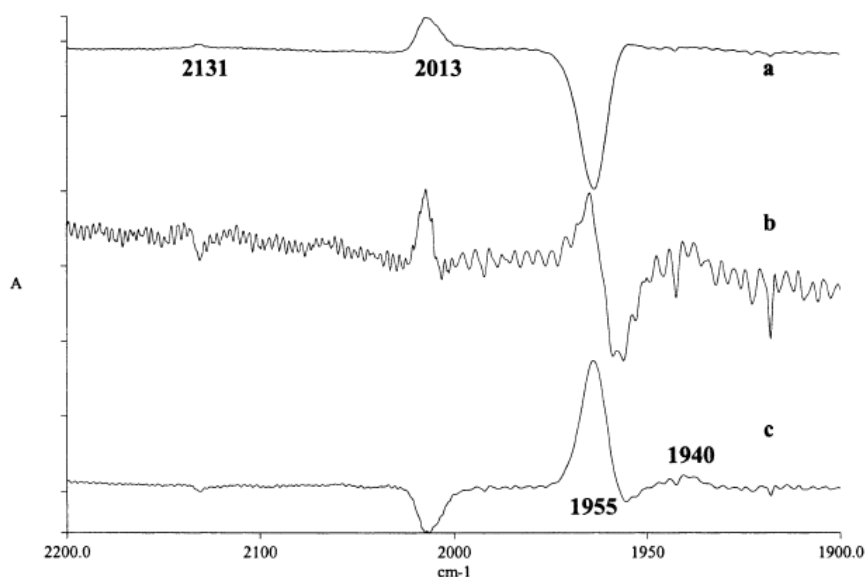


Fig. 5. (a) 4.5 h photolysis of **1**,  $\lambda_{\text{irr}} = 280 \pm 10$  nm. (b) Anneal to 130 K. (c) Anneal to 170 K.

To clarify the identity of the new species,  $^{13}\text{CO}$  labelled **1** (about 90% enrichment that also contains a trace of  $^{13}\text{C}^{18}\text{O}$ ) was prepared and photolyzed ( $330 < \lambda_{\text{irr}} < 400$  nm, 15 min) (Fig. 3b). Bands of **1** (1962  $\text{cm}^{-1}$ ), **1**- $^{13}\text{CO}$  (1916  $\text{cm}^{-1}$ ), and **1**- $^{13}\text{C}^{18}\text{O}$  (1873  $\text{cm}^{-1}$ ) were found to decrease while new bands at 2082, 2011, 1968, 1954, 1908, and 1865  $\text{cm}^{-1}$  were found to grow in. The observed bands at 1908 and 1865  $\text{cm}^{-1}$  correspond to the  $^{13}\text{CO}$  and  $^{13}\text{C}^{18}\text{O}$  labeled analogues of the species at 1955  $\text{cm}^{-1}$ , while the band at 1968  $\text{cm}^{-1}$  corresponds to the  $^{13}\text{CO}$  labeled analogue

of the previously observed band at  $2012\text{ cm}^{-1}$ . The band at  $2082\text{ cm}^{-1}$  is ‘free’  $^{13}\text{CO}$  in the Nujol glass matrix. Free  $^{12}\text{CO}$  and  $^{13}\text{C}^{18}\text{O}$  were not detectable above the background noise.

In 2-methyltetrahydrofuran glass at ca. 90 K, **1** has a slightly broadened band at  $1961\text{ cm}^{-1}$ . Photolysis of this band at energies as low as 500 nm resulted in a decrease in the bands of **1** and growth of a band at  $1952\text{ cm}^{-1}$ . Higher energy photolysis resulted in CO loss, but no new bands were observed.

Photolysis ( $350 < \lambda_{\text{irr}} < 400\text{ nm}$ , 30 min) of a frozen Nujol glass sample of **2** resulted in a decrease in the band of **2** ( $1954\text{ cm}^{-1}$ ) and growth of a new band at  $1947\text{ cm}^{-1}$ . No free CO was observed under these conditions. Further photolysis of this sample ( $330 < \lambda_{\text{irr}} < 400\text{ nm}$ , 30 min) resulted in a substantial bleaching of the band of **2** and appearance of a band at  $2130\text{ cm}^{-1}$ . No other product bands were observed.

Photolysis of **3** in frozen Nujol at  $\lambda_{\text{irr}} > 400\text{ nm}$  resulted in no apparent change in the IR spectral bands of **3** at  $2080$  and  $2000\text{ cm}^{-1}$ . Photolysis ( $330 < \lambda_{\text{irr}} < 400\text{ nm}$ , 15 min) resulted in a decrease in the bands of **3** and growth of bands at  $2131$ ,  $1977$ , and  $1960\text{ cm}^{-1}$  (Fig. 6).

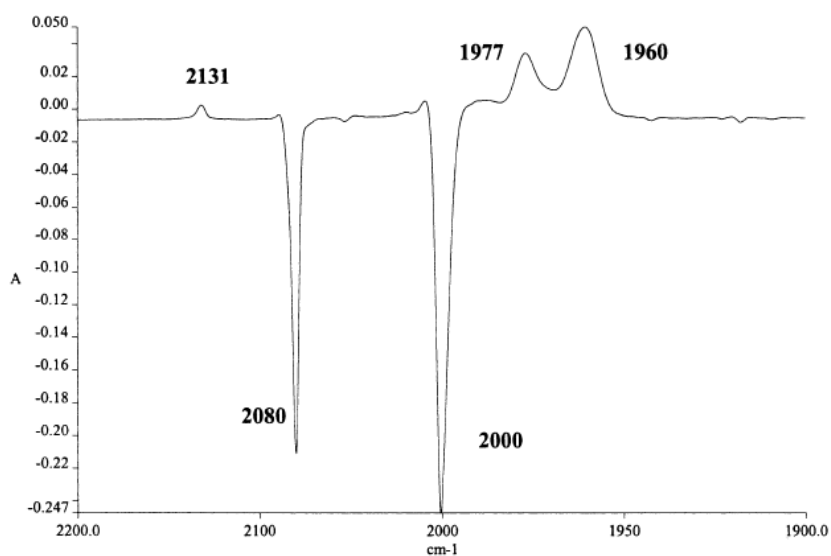


Fig. 6. 15 min photolysis of **3**,  $330 < \lambda_{\text{irr}} < 400\text{ nm}$ .

Photolysis of a sample of **4** containing a trace of **3** in frozen Nujol at  $\lambda_{\text{irr}} > 400$  nm exhibited no apparent change. Higher energy photolysis ( $330 < \lambda_{\text{irr}} < 400$  nm, 15 min) resulted in a decrease in the band of **4** and the appearance of a new band at  $2131\text{ cm}^{-1}$ . No other spectral features attributable to photoproducts of **4** were observed.

Summarizing our photochemical observations, low energy photolysis of both **1** and **2** result in the appearance of a new species, **A**, with IR bands slightly below those of the parent species. No such photoproduct was observed in the photolysis of the bis(amine) derivative **4**. Medium energy photolysis,  $330 < \lambda_{\text{irr}} < 400$  nm, of **1**, **2**, and **4** result in loss of CO to yield an IR silent photoproduct presumed to be  $\text{RhL}_2\text{Cl}$ . In addition, a new species with a carbonyl band at  $2012\text{ cm}^{-1}$ , **B**, is observed to form in both the medium and the high energy photolysis of **1**. Interestingly at the highest energies investigated,  $\lambda = 280 \pm 10$  nm, **B** appears to be the dominant product with relatively no CO loss as evidenced by the small bands at  $2131\text{ cm}^{-1}$ . **B** also appears upon annealing of matrices that have been photolyzed at high energy and thus contain free CO. **B** is converted to **1** by either annealing or long wavelength back photolysis. Finally, a species with an IR band at  $1938\text{ cm}^{-1}$ , **C**, appears on extended, low energy photolysis of **1** or upon annealing of matrices containing **A**. At long wavelength irradiation relatively little **C** is formed, but the relative amounts of this species increase with photolysis in the near UV. Interestingly, photolysis at 280 nm yields very little of either **A** or **C**. No bands comparable to **B** or **C** were observed in the photolysis of **2**. Photolysis of the mono(amine) derivative, **3**, results in loss of CO and appearance of two new carbonyl bands.

In an effort to clarify the identities of the various species present in the photolysis of **1** an effort was made to prepare and isolate *cis*- $\text{Rh}(\text{CO})_2(\text{PMe}_3)\text{Cl}$ . Trimethylphosphine was slowly added to a solution of  $\text{Rh}_2(\text{CO})_4\text{Cl}_2$  in petroleum ether under CO as described by Poliblanco and co-workers [13] with the formation of  $\text{Rh}(\text{CO})_2(\text{PMe}_3)\text{Cl}$  being confirmed by the appearance of

carbonyl bands at 2093 and 2001  $\text{cm}^{-1}$ . A CO saturated solution was stored at  $-78\text{ }^{\circ}\text{C}$  for several days during which time cherry red crystals appeared. All attempts to isolate these crystals resulted in a rapid color change from bright red to dull tan. The resulting tan product was shown by IR to be  $\text{Rh}_2(\text{CO})_2(\text{PMe}_3)_2(\mu\text{-Cl})_2$ . We believe that the red crystals are  $\text{Rh}(\text{CO})_2(\text{PMe}_3)\text{Cl}$  and attribute their color to the well known d-d stacking effects observed for some  $\text{Rh}(\text{CO})_2(\text{amine})\text{Cl}$  derivatives [11,14]. When petroleum ether solutions containing  $\text{Rh}(\text{CO})_2(\text{PMe}_3)\text{Cl}$  were frozen to liquid nitrogen temperatures a purple color was observed that we believe to be due to continued growth of d-d stacks at low temperature.

### 3. Discussion

The lowest energy photoproduct, **A**, of **1** and **2** forms upon photolysis into the bottom edge of the 360 nm band without loss of CO. In our preliminary analysis of these spectra we speculated that it might arise from loss of a  $\text{PMe}_3$  ligand as has been reported by Perutz and coworkers [15] for *cis*- $\text{Ru}(\text{PMe}_3)_4\text{H}_2$ . Reinforcing this hypothesis was the similarity of the IR band of  $[\text{Rh}(\text{CO})(\text{PMe}_3)_3]\text{Cl}$  with that of **C**.

Our attempts to prepare and isolate  $\text{Rh}(\text{CO})_2(\text{PMe}_3)\text{Cl}$  as a precursor to the putative  $[\text{Rh}(\text{CO})(\text{PMe}_3)\text{Cl}]$  intermediate proved unsuccessful, thus we opted to prepare a corresponding ammine series of derivatives to serve as analogues. The choice of ammine in this case was dictated by our desire for a comparatively simple ligand, but also one that would preclude d-d stacking of the square-planar rhodium molecules. Our first choice for a model compound was the previously unknown  $\text{Rh}(\text{CO})_2(\text{Et}_3\text{N})\text{Cl}$ . While this compound was easily formed upon addition of  $\text{Et}_3\text{N}$  to  $\text{Rh}_2(\text{CO})_4(\mu\text{-Cl})_2$ , it proved to be exceptionally air-sensitive giving rise to a blue species, we believe to be an  $\text{O}_2$  adduct. It appears that there has only been one other report of an

attempted synthesis of  $\text{Rh}(\text{CO})_2\text{LCl}$  derivatives with tertiary amines and these compounds were simply described as being unstable [16]. Although we were ultimately able to carry out Nujol matrix studies on  $\text{Rh}(\text{CO})_2(\text{NEt}_3)\text{Cl}$  that parallel the results for the di(isopropyl)amine derivative described below, the quality of these spectra were not high and it was clear that impurities were present.

As an alternative to  $\text{Rh}(\text{CO})_2(\text{Et}_3\text{N})\text{Cl}$ , the known, air-stable derivative  $\text{Rh}(\text{CO})_2(i\text{-Pr}_2\text{HN})\text{Cl}$  (**3**), was prepared. Compound **3** is known to exist in the solid state and in solution as a monomeric species [11]. IR bands of **3** are observed in Nujol at 2080 and 2000  $\text{cm}^{-1}$ , somewhat lower in energy than  $\text{Rh}(\text{CO})_2(\text{PMe}_3)\text{Cl}$  in CO saturated petroleum ether for which bands are observed at 2094 and 2001  $\text{cm}^{-1}$ .

Photolysis of **3** is expected to give rise to two isomeric carbonyl loss products (Fig. 7) as is observed. Chloride is a potential  $\pi$ -electron donor while there can be no comparable donation from the ammine ligand. Accordingly, we have assigned the photoproduct with the lower carbonyl stretching frequency (1960  $\text{cm}^{-1}$ ) to the isomer with the carbonyl trans to the chloride, and the species with the higher carbonyl stretching frequency (1977  $\text{cm}^{-1}$ ) to the isomer with the carbonyl *trans* to the ammine.

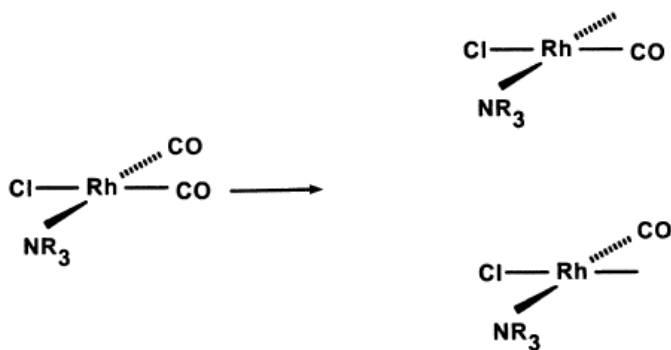
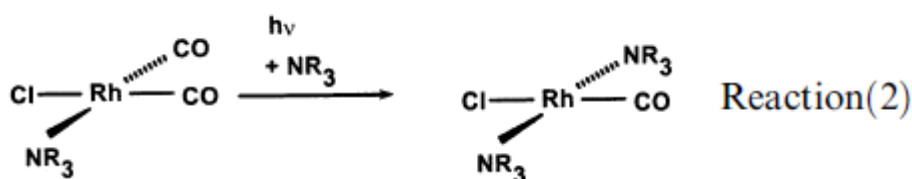


Fig. 7. CO-loss isomeric photoproducts of  $\text{Rh}(\text{CO})_2(\text{amine})\text{Cl}$  derivatives.

Photolysis of **3** in heptane with an excess of di(isopropyl) amine resulted in formation of **4** along with a dark decomposition product, Reaction (2). The carbonyl stretching band of **4** is found at  $1940\text{ cm}^{-1}$  in Nujol while the comparable band of **1** appears at  $1962\text{ cm}^{-1}$ . The differences in carbonyl stretching frequencies are readily explained by the difference in  $\pi$ -acidic character of the two ligands. The ammine has no  $\pi$ -acidic character thus backbonding transfers more metal electron density to the carbonyl ligand in the ammine derivative than in the phosphine case. Matrix photolysis of **4** indicates that CO is lost at high energy, but there are no other intermediates analogous to those observed for **1** or **2**. We are presently exploring the solution photochemistry of **4** and other bis(ammine) derivatives.



By analogy with the carbonyl stretching frequencies of **1** and **4** we would anticipate the putative  $\text{PMe}_3$ -loss intermediate  $[\text{Rh}(\text{CO})(\text{PMe}_3)\text{Cl}]$  to have a carbonyl stretching frequency ca.  $22\text{ cm}^{-1}$  above that of its ammine analogue ( $1960\text{ cm}^{-1}$ ) or about  $20\text{ cm}^{-1}$  above that of **1**. DFT calculations on **1** and  $[\text{Rh}(\text{CO})(\text{PMe}_3)\text{Cl}]$  predict the monophosphine species to have a carbonyl stretching frequency  $29\text{ cm}^{-1}$  above that of **1**. This is remarkably consistent with our prediction above. We note that  $[\text{Rh}(\text{CO})(i\text{-Pr}_2\text{HN})\text{Cl}]$  has a carbonyl stretching frequency  $20\text{ cm}^{-1}$  above that of  $\text{Rh}(\text{CO})(i\text{-Pr}_2\text{HN})_2\text{Cl}$ . These data are summarized in Fig. 8. Based on this analysis, we must conclude that the photoproduct **A** cannot be assigned to the phosphine loss species  $[\text{Rh}(\text{CO})(\text{PMe}_3)\text{Cl}]$ .

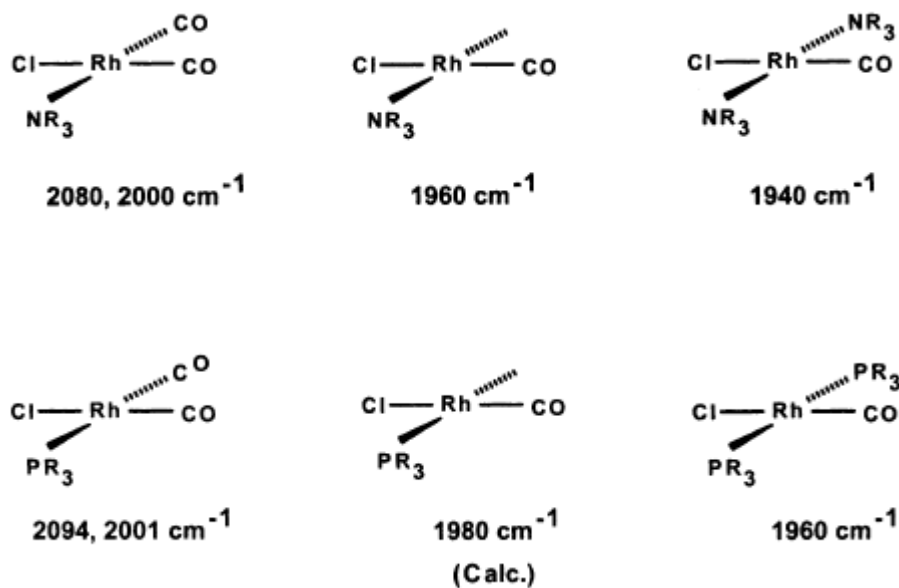


Fig. 8. Summary of observed and calculated rhodium carbonyl phosphine and ammine derivatives.

Brady *et al.* have reported electronic spectral studies on a series of square-planar complexes of the form  $M(\text{CO})\text{L}_2\text{Cl}$ , where  $M = \text{Rh}$  and  $\text{Ir}$ , and  $\text{L} = \text{PR}_3$ , where  $\text{R} = \text{alkyl and aryl groups}$  [17]. It was noted that electronic transitions at 360 nm sharpened when observed at 77 K, but the reported measurements did not extend below 300 nm, thus the 275 nm feature observed in the current work was not seen. Brady *et al.* attribute the 360 nm transition to an  $a_1(z^2)-b_1\pi$  (HOMO-LUMO) transition with MLCT character. The second highest excitation would be  $a_1(z^2)-a_1(x^2-y^2)$ . Since the latter orbital is antibonding with respect to the ligands it may well be associated with the higher energy CO-loss excitation. The electronic spectra of the  $C_{2v}$   $M(\text{CO})\text{L}_2\text{Cl}$  species parallel to those observed for  $D_{4h}$   $[\text{M}(\text{PC}_2\text{P})_2]^{+1}$  and  $[\text{M}(\text{PC}=\text{CP})_2]^{+1}$  complexes and are typically interpreted by analogy to the more symmetric case (Fig. 9). Geoffroy *et al.* [18] and Fordyce and Crosby [19] have noted that the lower energy transition of the complexes with  $D_{4h}$  symmetry is  $^1\text{A}_{1g}-^3\text{A}_{2u}$  ( $a_{1g}-a_{2u}$ ), while the next higher energy band is  $^1\text{A}_{1g}-^1\text{A}_{2u}$  ( $a_{1g}-a_{2u}$ ). It is interesting to note that large Stokes shifts observed in the emission spectra of  $\text{Rh}(\text{I})$   $D_{4h}$  complexes have been

interpreted to suggest substantial distortion of the excited states. Geoffroy et al. [18] propose that the emitting state is not purely MLCT in character, but includes one or more d-d states leading to a tetrahedral distortion. We shall return to this point below.

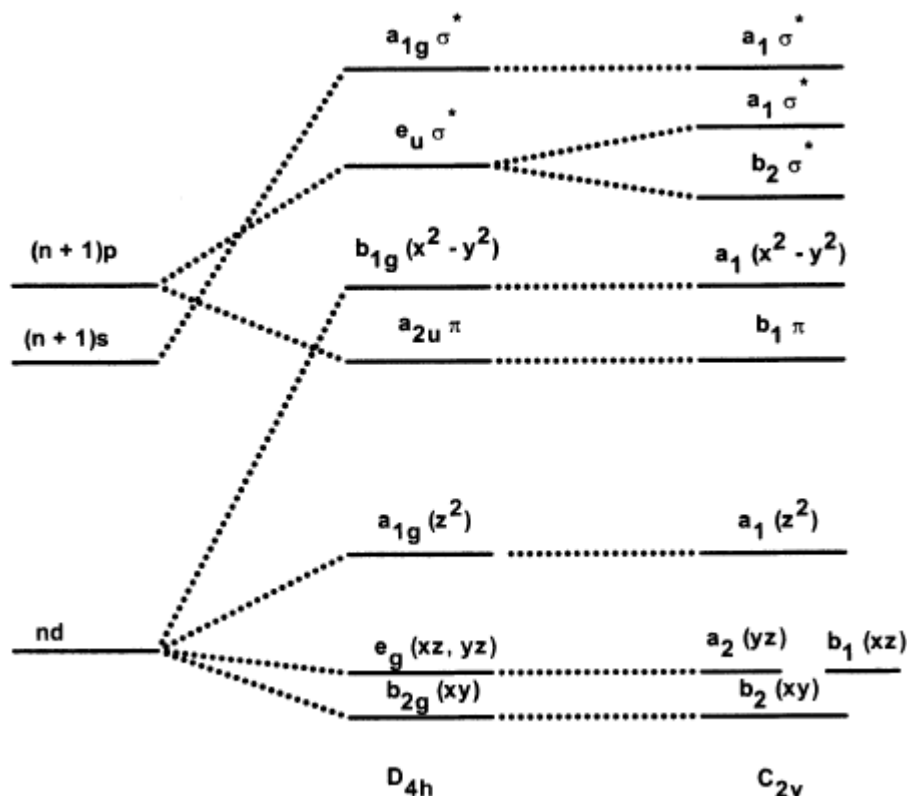


Fig. 9. Molecular orbital energy level diagram (ref. [17]).

As noted above, spectral studies on Rh(I) complexes have suggested that the lowest energy electronic transition is consistent with a triplet excited state, and that some evidence exists to suggest that this excited state deviates from square-planar geometry. We have carried out density functional theory (DFT) calculations of **1** and its  $PH_3$  model compound in an attempt to better understand the nature of this excited state. Calculated bond lengths and angles for  $Rh(CO)(PH_3)_2Cl$  and **1** are presented in Tables 1 and 2 along with crystallographically derived

values for **1**. The calculated structures are presented in Fig. 10. Calculated energies and CO stretching frequencies are presented in Table 3.

$\text{Rh}(\text{CO})(\text{PH}_3)_2\text{Cl}$  was found to have two excited state, triplet geometries: a distorted-planar geometry that lies  $36.4 \text{ kcal mol}^{-1}$  above the ground state and a nonplanar geometry in which the chloride ligand has moved out of the molecular plane that is  $30.8 \text{ kcal mol}^{-1}$  above the ground state. The geometries of these triplet species are presented in Fig. 10. These very surprising results prompted us to carry out calculations on **1** itself, for which we found a non-planar triplet excited state  $35.3 \text{ kcal mol}^{-1}$  above the ground state. Like the  $\text{PH}_3$  case, the chloride ligand was found to have moved out of the molecular plane. Bond lengths and angles of the three triplet species are given in Table 1. Calculations of the IR frequencies of both the ground and excited states were carried out and these values are presented in Table 3. The calculated ground state vibrational frequency is  $1912 \text{ cm}^{-1}$  and the frequency of the triplet species is calculated to be about  $1.5 \text{ cm}^{-1}$  below this. DFT calculated absolute values of vibrational frequencies for metal complexes are often observed to be shifted to lower energy and calculations on excited state species are particularly difficult. For this reason we note that calculations lend cautious support to the assignment of the species observed at  $1955 \text{ cm}^{-1}$  to a non-squareplanar triplet which is stabilized by the low temperatures and relatively inert matrix. This is consistent with the ease of conversion of this species to the starting material upon annealing.

Table 1. Calculated bond lengths ( $\text{\AA}$ ) and angles ( $^\circ$ ) for  $\text{Rh}(\text{CO})(\text{PH}_3)_2\text{Cl}$

	Singlet	Triplet, non-planar	Triplet, planar
<i>Bond lengths</i>			
Rh-P	2.393	2.537	2.735
Rh-Cl	2.447	2.515	2.514
Rh-C	1.842	1.925	1.935
C-O	1.187	1.181	1.179
<i>Bond angles</i>			

Cl-Rh-P	84.59	86.74	79.13
Cl-Rh-C	180.00	108.61	179.98
P-Rh-P	169.18	153.60	158.25
P-Rh-C	95.42	103.16	100.87
Rh-C-O	179.98	175.71	180.00

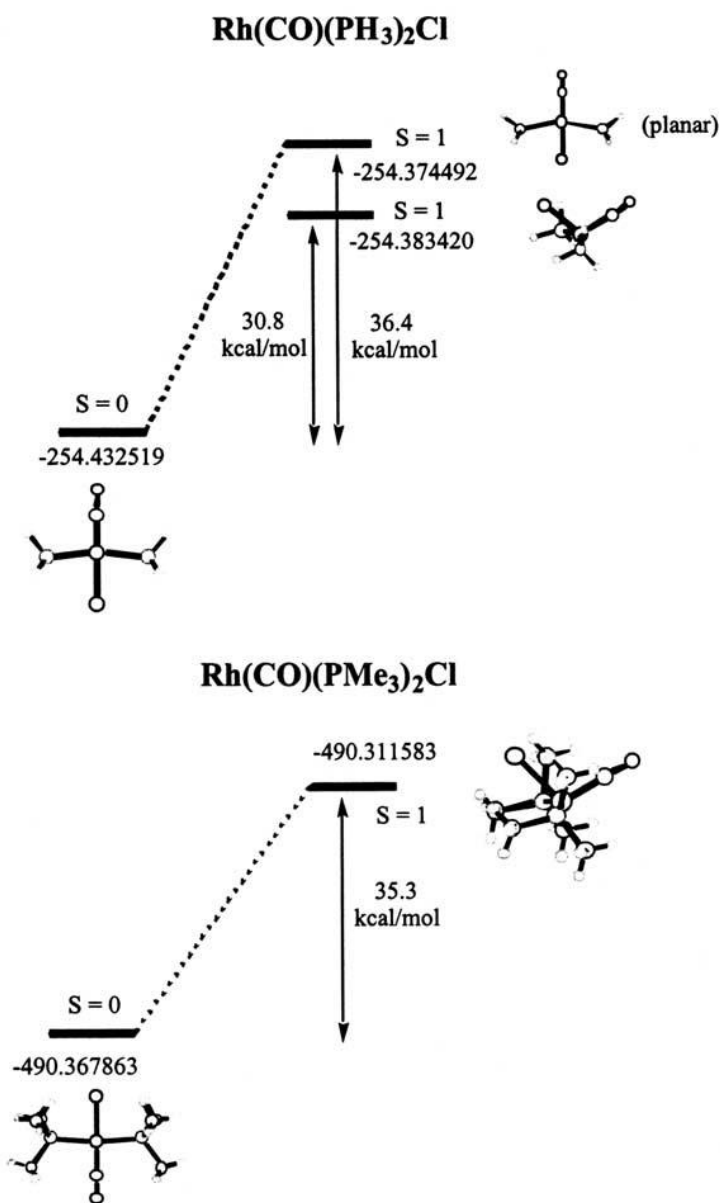


Fig. 10. Computed geometries and energies for Rh(CO)(PH<sub>3</sub>)<sub>2</sub>Cl, Rh(CO)(PMe<sub>3</sub>)<sub>2</sub>Cl and their related planar and non-planar triplet excited states.

The data from both photolysis and annealing experiments suggest that **C** either arises as a secondary photolysis product of **A** or through warming of **A**. **C** is unaffected by annealing to as

high as 170 K. The identity of this species is an enigma to us as an oxidative addition reaction between the metal and Nujol or a  $\text{PMe}_3$  ligand would yield a Rh(III) species that should exhibit higher carbonyl frequencies, not lower frequencies. The dilution of **1** in the Nujol matrices is sufficiently high as such we do not believe that intermolecular interactions between rhodium molecules can account for the observed bands.

High energy photolysis of **1** gives rise to CO-loss as well as to the appearance of a new species, **B**, with a carbonyl band at  $2012\text{ cm}^{-1}$ . **B** is transformed to **1** by back photolysis. It is significant that **B** also appears upon annealing of a matrix that had been photolyzed at high energy and thus contained both free CO and the IR silent  $\text{Rh}(\text{PMe}_3)_2\text{Cl}$  species. No such species is observed for **2** or for **4**.

Recapture of a CO by  $\text{Rh}(\text{PMe}_3)_2\text{Cl}$  results in reformation of **1**, but could also give rise to the *cis* isomer of this compound. The *cis* isomer would be expected to be thermally and photochemically unstable and revert to the *trans* isomer as is observed. Failure to observe comparable bands in the photolysis of **2** may be due to the steric bulk of the tributylphosphine ligands making a *cis* isomer highly unstable. At very high energies it appears that **B** can form directly from **1**, possibly through a tetrahedral excited state.

As noted in Section 1, Ford and co-workers [7a] has used time-resolved IR to study the photolysis of **1** in benzene. Two bands observed at  $2130$  and  $2018\text{ cm}^{-1}$  in  $\text{C}_6\text{H}_6$  were assigned to metal hydride bands. These bands were absent when the photolyses were carried out in  $\text{C}_6\text{D}_6$ . We suggest that the band observed at  $2130\text{ cm}^{-1}$  may be attributable to free CO and it is likely that the  $2018\text{ cm}^{-1}$  band is due to the same photoproduct observed in these matrix studies. Indeed, we have observed a species at  $2019\text{ cm}^{-1}$  in a time-resolved IR study, the photolysis of **1** in supercritical  $\text{CO}_2$  [20]. The band at  $2019\text{ cm}^{-1}$  decays slightly within the 150 ms time frame of the

experiment. We must regard these interpretations as preliminary as we have no explanation for why these bands were not observed in the deuterated solvent.

To further clarify the identity of the 2012  $\text{cm}^{-1}$  species we have carried out DFT calculations on *cis*-Rh(CO)(PMe<sub>3</sub>)<sub>2</sub>Cl and found that this isomer is expected to have a carbonyl stretching frequency 41  $\text{cm}^{-1}$  higher than that of the *trans* isomer. This yields a predicted value of 2003  $\text{cm}^{-1}$  that is in good agreement with the observed values of 2012-2018  $\text{cm}^{-1}$ . Representative calculated bond lengths and angles for the *cis* isomer are presented in Table 2. The difference in carbonyl stretching frequency between the *cis* and *trans* isomers may be readily attributed to the carbonyl group being *trans* to a  $\pi$ -donor chloride in **1** and *trans* to a weak  $\pi$ -acid trimethylphosphine in the *cis* isomer.

Table 2. Calculated and experimental bond lengths (Å) and angles (°) for **1**, its non-planar triplet, *cis* isomer and PMe<sub>3</sub> loss species, Rh(CO)(PMe<sub>3</sub>)Cl

	<b>1</b> , cal.	<b>1</b> , exp. Ref. [26]	Non-planar triplet	<i>cis</i> -Rh(CO)(PMe <sub>3</sub> )Cl	Rh(CO)(PMe <sub>3</sub> )Cl
<i>Bond lengths</i>					
Rh-P	2.412	2.308	2.512	2.38 (cis-CO) 2.498 (trans-CO)	2.3887
Rh-Cl	2.471	2.354	2.556	2.4588	2.3887
Rh-C	1.829	1.770	1.920	1.8592	1.8444
C-O	1.191	1.146	1.185	1.1822	1.1876
<i>Bond angles</i>					
Cl-Rh-P	85.66	88.7	87.30	180.03	
Cl-Rh-C	179.98	179.4	106.28	87.59	177.63
P-Rh-P	171.31	177.2	155.21	97.90	
P-Rh-C	94.34	91.3	102.37	180.04 (trans ) 92.14 (cis )	
Rh-C-O	179.97	178.4	179.51	179.56	179.49

#### 4. Conclusions

Solution photochemical studies of **1** by Ford and coworkers [7] and Rosini et al. [8] have provided evidence for the existence of two photochemical pathways in the oxidative addition of hydrocarbons, one involving CO loss and a second involving direct interaction of an excited state of **1** with hydrocarbon. Our matrix studies now provide support for the existence of three distinct photochemical processes: (a) serendipitous observation of a low energy excited triplet, or perhaps a rearranged and stabilized isomer of this species, (b) CO-loss, and (c) direct, high energy formation of the *cis*-Rh(CO)(PMe<sub>3</sub>)<sub>2</sub>Cl isomer. The *cis*-Rh(CO)(PMe<sub>3</sub>)<sub>2</sub>Cl isomer may also be formed by recapture of CO by Rh(PMe<sub>3</sub>)<sub>2</sub>Cl. The identity of a further species that appears to be formed from the low energy photointermediate remains unknown.

Finally, it is important to note that the energy range necessary for direct *trans* to *cis* conversion of **1** corresponds to that described by Rosini et al. [8] as being associated with oxidative addition of benzene to the intact excited state of **1**. In both cases these processes would appear to be triggered by photolysis into the electronic band with a maxima at 275 nm.

Table 3. Calculated and experimental bond lengths (Å) and angles (°) for **1**, its non-planar triplet, *cis* isomer and PMe<sub>3</sub> loss species, Rh(CO)(PMe<sub>3</sub>)Cl

	R = H		R = CH <sub>3</sub>		
	<i>E</i> (kcal mol <sup>-1</sup> )	νCO (cm <sup>-1</sup> )	<i>E</i> (kcal mol <sup>-1</sup> )	νCO (cm <sup>-1</sup> ) (cal)	νCO (cm <sup>-1</sup> ) (obs)
Rh(CO)(PR <sub>3</sub> ) <sub>2</sub> Cl, singlet	0	1939.06	0	1911.95	1962
Rh(CO)(PR <sub>3</sub> ) <sub>2</sub> Cl, triplet, planar	36.4	1955.73			
Rh(CO)(PR <sub>3</sub> ) <sub>2</sub> Cl, triplet, non-planar	30.8	1937.59	35.3	1910.58	1955
<i>cis</i> -Rh(CO)(PR <sub>3</sub> ) <sub>2</sub> Cl			13.7	1952.1	2012
Rh(CO)(PR <sub>3</sub> )Cl			35.66	1930.2	

## 5. Experimental

Compounds **1** [8], **2** [10], and **3** [11] were prepared by standard literature procedures. The details of the preparation of **4** and other bis(ammine) derivatives will be presented elsewhere [12]. Electronic spectra were recorded on a Cary 2200 Spectrometer. IR spectra were recorded using a Perkin-Elmer Spectrum 1000 FTIR Spectrometer. IR spectra were recorded at 4 cm<sup>-1</sup> resolution. Nujol matrix studies were carried out using a cryostat designed by Dr. A. Rest of the University of Southampton. 2-Methyltetrahydrofuran matrix studies were carried out using a Graseby Specac Variable Temperature Cryostat. Photolyses were carried out using a 350 W high pressure Hg lamp. Optical filters were used to control the wavelength ranges of the incident radiation.

## 6. Computational details

All systems have been studied using the B3LYP hybrid density functional theory [21], which has proven to be very reliable for a broad range of organometallic systems similar to those reported here [22]. All geometry optimizations and frequency calculations were carried out with the GAUSSIAN 98 program package [23] using the standard LanL2DZ basis set, which includes both Dunning and Hay's D95 sets for H and C [24] and the relativistic core potential sets of Hay and Wadt for the heavy atoms [25]. The input geometry for the singlet *trans*-Rh(CO)(PH<sub>3</sub>)<sub>2</sub>Cl and *trans*-Rh(CO)(PMe<sub>3</sub>)<sub>2</sub>Cl molecules were adapted from the published X-ray structure of the PMe<sub>3</sub> complex [26]. The corresponding triplet structures were obtained starting from a pseudotetrahedral input geometry with bond distances set to those obtained from the corresponding singlet optimization. A different, higher energy local minimum having a planar geometry was obtained for the PH<sub>3</sub> model compound when starting from the optimized planar geometry of the singlet state. For the larger PMe<sub>3</sub> molecule, this calculation was not carried out.

All calculations were carried out without imposed symmetry. Spin contamination was carefully monitored and the value of  $\langle S^2 \rangle$  for the unrestricted B3LYP calculations on the triplet states at convergence [2.0076 for  $\text{RhCl}(\text{CO})(\text{PH}_3)_2$ ; 2.0083 for  $\text{RhCl}(\text{CO})(\text{PMe}_3)_2$ ] indicated minor spin contamination. The energies reported in Sections 2 and 3 do not include a correction for zero-point energy.

## Acknowledgements

T.E.B. wishes to thank the Research Corporation for their generous award of a Research Opportunity grant and the Pacific Northwest National Laboratory for financial support. We thank Professor Goldman for his generous gift of our first samples of **1**, and Dr. G. Rosini, Professor Goldman and Professor Ford for helpful advice. We sincerely thank a referee for pointing out the probable direct formation of **B** from **1** at high energy.

## References

- [1] T.E. Bitterwolf, D.L. Kline, J.C. Linehan, C.R. Yonker, R.S. Addleman, *Angewandte Chemie* 113 (2001) 2764.
- [2] J.-C. Choi, Y. Kobayashi, T. Sakakura, *J. Organic Chem.* 66 (2001) 5262.
- [3] (a) B.J. Fisher, R. Eisenberg, *Organometallics* 2 (1983) 764; (b) A.J. Kunin, R. Eisenberg, *J. Am. Chem. Soc.* 108 (1986) 535; (c) A.J. Kinin, R. Eisenberg, *Organometallics* 7 (1988) 2124; (d) E.M. Gordon, R. Eisenberg, *J. Mol. Catal.* 45 (1988) 57.
- [4] (a) T. Sakakura, T. Sodeyama, K. Sasaki, K. Wada, M. Tanaka, *J. Am. Chem. Soc.* 112 (1990) 721; (b) M. Tanaka, T. Sakakura, *Pure Appl. Chem.* 62 (1990) 1147; (c) T. Sakakura, K. Sasaki, Y. Tokunaga, K. Wada, M. Tanaka, *Chem. Lett.* (1988) 155; (d) T. Sakakura, M. Tanaka, *J. Chem. Soc. Chem. Commun.* (1987) 758; (e) T. Sakakura, M. Tanaka, *Chem. Lett.* (1987) 1113; (f) T. Sakakura, M. Tanaka, *Chem. Lett.* (1987) 249.
- [5] W.T. Bowse, A.S. Goldman, *J. Am. Chem. Soc.* 114 (1992) 350.
- [6] (a) G.P. Rosini, S. Soubra, M. Vixamar, S. Wang, A.S. Goldman, *J. Organometal. Chem.* 554 (1998) 41; (b) J.A. Maguire, W.T. Boese, A.S. Goldman, *J. Am. Chem. Soc.* 111 (1989) 7088; (c) J.A. Maguire, A.S. Goldman, *J. Am. Chem. Soc.* 113 (1991) 6706.
- [7] (a) J.S. Bridgewater, B. Lee, S. Bernhard, J.R. Schoonover, P.C. Ford, *Organometallics* 16 (1997) 5592; (b) C.T. Spillett, P.C. Ford, *J. Am. Chem. Soc.* 111 (1989) 1932; (c) D.A. Wink, P.C. Ford, *J. Am. Chem. Soc.* 109 (1987) 436; (d) D. Wink, P.C. Ford, *J. Am. Chem. Soc.* 107 (1985) 1794.

- [8] G.P. Rosini, W.T. Boese, A.S. Goldman, *J. Am. Chem. Soc.* 116 (1994) 9498.
- [9] (a) T.E. Bitterwolf, K.A. Lott, A.J. Rest, J. Mascetti, *J. Organomet. Chem.* 419 (1991) 113; (b) R.H. Hooker, A.J. Rest, *J. Chem. Soc. Dalton Trans.* (1984) 761.
- [10] R.F. Heck, *J. Am. Chem. Soc.* 86 (1964) 2796.
- [11] (a) L.M. Vallarino, S.W. Sheargold, *Inorg. Chim. Acta* 36 (1979) 243; (b) D.N. Lawson, G. Wilkinson, *J. Chem. Soc.* (1965) 1900.
- [12] T.E. Bitterwolf, manuscript in preparation, 2001.
- [13] (a) E. Rotondo, G. Battaglia, G. Giordano, F.P. Cusmano, *J. Organomet. Chem.* 450 (1993) 245; (b) R. Poliblanco, *J. Organomet. Chem.* 94 (1975) 241; (c) J. Gallay, D. De Montauzon, R. Poliblanco, *J. Organomet. Chem.* 38 (1972) 179.
- [14] (a) M.C. Torralba, M. Cano, J.A. Campo, J.V. Heras, E. Pinilla, M.R. Torres, *J. Organomet. Chem.* 633 (2001) 91; (b) T.W. Thomas, A.E. Underhill, *J. Chem. Soc. Rev.* 1 (1972) 99.
- [15] V. Montiel-Palma, R.N. Perutz, M.W. George, O.S. Jina, S. Sabo-Etienne, *J. Chem. Soc. Chem. Commun.* (2000) 1175.
- [16] M.E. Krafft, L.J. Wilson, K.D. Onan, *Organometallics* 7 (1988) 2528.
- [17] R. Brady, B.R. Flynn, G.L. Geoffroy, H.B. Gray, J. Peone, Jr., L. Vaska, *Inorg. Chem.* 15 (1976) 1485.
- [18] G.L. Geoffroy, M.S. Wrighton, G.S. Hammond, H.B. Gray, *J. Am. Chem. Soc.* 96 (1975) 3105.
- [19] W.A. Fordyce, G.A. Crosby, *Inorg. Chem.* 21 (1982) 1455.
- [20] T.E. Bitterwolf, D.L. Kline, J.C. Linehan, C.R. Yonker, R.S. Addleman, manuscript in preparation, 2002.
- [21] A.D. Becke, *J. Chem. Phys.* 98 (1993) 5648.
- [22] S. Niu, M.B. Hall, *Chem. Rev.* 100 (2000) 353.
- [23] M.J. Frisch, G.W. Trucks, H.B. Schlegel, G.E. Scuseria, M.A. Robb, J.R. Cheeseman, V.G. Zakrzewski, J. Montgomery, J.A., R.E. Stratmann, J.C. Burant, S. Dapprich, J.M. Millam, A.D. Daniels, K.N. Kudin, M.C. Strain, O. Farkas, J. Tomasi, V. Barone, M. Cossi, R. Cammi, B. Mennucci, C. Pomelli, C. Adamo, S. Clifford, J. Ochterski, G.A. Petersson, P.Y. Ayala, Q. Cui, K. Morokuma, D.K. Malick, A.D. Rabuck, K. Raghavachari, J.B. Foresman, J. Cioslowski, J.V. Ortiz, A.G. Baboul, B.B. Stefanov, G. Liu, A. Liashenko, P. Piskorz, I. Komaromi, R. Gomperts, R.L. Martin, D.J. Fox, T. Keith, M.A. Al-Laham, C.Y. Peng, A. Nanayakkara, C. Gonzalez, M. Challacombe, P.M.W. Gill, B. Johnson, W. Chen, M.W. Wong, J.L. Andres, C. Gonzalez, M. Head-Gordon, E.S. Replogle, J.A. Pople, *Gaussian 98, Revision A.7*, Gaussian, Inc., Pittsburgh, PA, 1998.
- [24] T.H. Dunning, III, P.J. Hay, in: H.F. Schaefer III (Ed.), *Modern Theoretical Chemistry*, Plenum Press, New York 1976, p. 1.
- [25] (a) P.J. Hay, W.R. Wadt, *J. Chem. Phys.* 82 (1985) 270; (b) W.R. Wadt, P.J. Hay, *J. Chem. Phys.* 82 (1985) 284; (c) P.J. Hay, W.R. Wadt, *J. Chem. Phys.* 82 (1985) 299.
- [26] S.E. Boyd, L.D. Field, T.W. Hambley, M.G. Partridge, *Organometallic* 12 (1993) 1720.